

New Ru(II) Complexes Containing Oxazoline Ligands As Epoxidation Catalysts. Influence of the Substituents on the Catalytic Performance

Isabel Serrano,[†] M. Isabel López,[†] Ingrid Ferrer,[†] Albert Poater,[‡] Teodor Parella,[§] Xavier Fontrodona,[†] Miquel Solà,[†] Antoni Llobet,^{§,||} Montserrat Rodríguez,^{*,†} and Isabel Romero^{*,†}

[†]Departament de Química, Serveis Tècnics de Recerca and Institut de Química Computacional, Universitat de Girona, Campus de Montilivi, E-17071 Girona, Spain

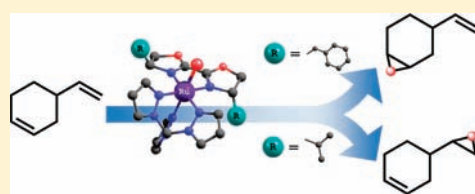
[‡]Catalan Institute for Water Research (ICRA), H₂O Building, Scientific and Technological Park of the University of Girona, Emili Grahit 101, E-17003 Girona, Spain

[§]Departament de Química and Servei de RMN, Universitat Autònoma de Barcelona, E-08193 Bellaterra, Barcelona, Spain

^{||}Institute of Chemical Research of Catalonia (ICIQ), Av. Països Catalans 16, E-43007 Tarragona, Spain

S Supporting Information

ABSTRACT: The synthesis of a family of new Ru complexes containing the facial tridentate ligand with general formula [Ru^{II}(T)(D)(X)]ⁿ⁺ (T = trispyrazolylmethane (tpm); D = ((4*S*,4'*S*)-(-)-4,4',5,5'-tetrahydro-4,4'-bis(1-methylethyl)-2,2'-bioxazole) (iPr-box-C) or *N*-(1-hydroxy-3-methylbutan-(2*S*)-(-)-2-yl)-(4*S*)-(-)-4-isopropyl-4,5-dihydrooxazole-2-carbimide (iPr-box-O); X = Cl, H₂O) has been described. All complexes have been spectroscopically characterized in solution through ¹H NMR and UV–vis techniques, and the redox properties of complexes have also been studied by means of cyclic voltammetry (CV). Furthermore, the chloro complexes presented here have been characterized in the solid state through monocrystal X-ray diffraction analysis. The oxazolinic iPr-box-O ligand undergoes a Ru-assisted hydrolysis reaction generating the corresponding amidate anionic ligand iPr-box-C, that keeps coordinated to the Ru metal center and that produces a strong σ -donation effect over it. The reactivity of the Ru–OH₂ complexes described in this paper together with other similar ones, previously synthesized by us, has been tested with regard to the epoxidation of different olefins. Complexes [Ru^{II}(R-box-C)(tpm)OH₂](BF₄)₂, R = Bz, 3'*c*/iPr, 3*c*, show high stereoselectivity in the epoxidation of *cis*- β -methylstyrene, with the exclusive formation of the *cis*-epoxide. However, there is a significant difference in regioselectivity between the two catalysts in the epoxidation of 4-vinylcyclohexene; complex 3'*c* leads to the regioselective oxidation at the ring alkene position, whereas complex 3*c* leads to the oxidation at the terminal position. Computational calculations indicate only small energy differences between the two possible products of 4-vinylcyclohexene epoxidation, but the energy barriers for the interaction of the catalytic systems with the alkene groups of 4-vinylcyclohexene agree with the reactivity differences found for the two catalysts having isopropyl or benzyl as substituent of the oxazole ligand. Computed local Fukui functions help to explain the observed reactivity trends.

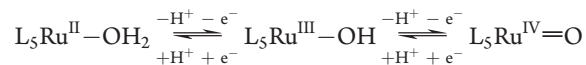


INTRODUCTION

Metal-catalyzed oxidation is one of the most important atom transfer reactions in chemistry and biology.¹ Olefin epoxidation has received considerable interest from both academics and industry; specifically, enantiomerically pure epoxides play an eminent role as intermediates and building blocks in organic synthesis and materials science.² Although numerous procedures have been developed, the need for understanding the mechanisms of metal-mediated oxygen processes demands the synthesis of new, stable, and easily available catalysts.

In the field of redox catalysis, the relationship between performance and structure of a catalyst is further complicated by the presence of multiple redox state species involved in the catalytic cycle. Therefore, the thermodynamic and kinetic characterization of the reactions that undergo the different oxidation state species of a particular catalyst is of paramount importance to understand and optimize its performance.

A particularly interesting family of redox catalysts is the so-called Ru–OH₂ type of complexes. These Ru-aquo complexes can easily lose protons and electrons and reach higher oxidation states as exemplified below, where L₅ represents polypyridylic type of ligands,

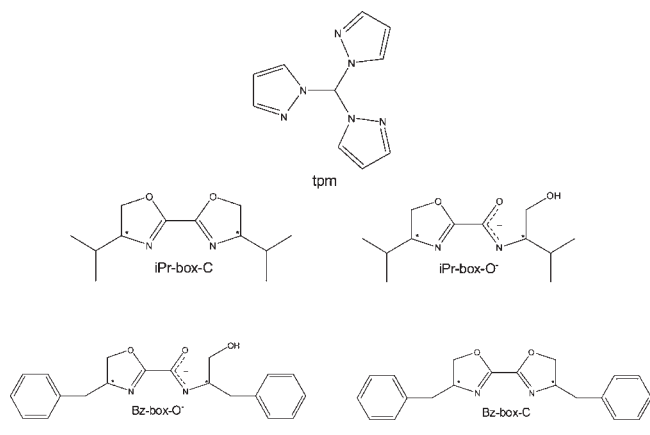


The sequential loss of protons and electrons allows to easily reach reactive Ru^{IV}=O species and as a consequence these Ru complexes have been widely used as redox catalysts for the oxidation of both organic and inorganic substrates. A large amount of literature has emerged during the past two decades related to this system, mainly because of the rich oxidative

Received: January 9, 2011

Published: June 08, 2011

Chart 1. Drawing of Ligands Used in This Work



properties of the $\text{Ru}^{\text{IV}}=\text{O}$ species. In addition, the reaction mechanisms for the oxidation of several substrates by $\text{Ru}^{\text{IV}}=\text{O}$ have been thoroughly described together with the establishment and optimization of catalytic processes.³

The redox potentials and, therefore, the performance of a $\text{Ru}-\text{OH}_2$ catalyst can be fine-tuned through the addition of electron donating or withdrawing groups to the ligands. These are expected to respectively decrease and increase the $\text{Ru}(\text{IV})/\text{Ru}(\text{III})$ and $\text{Ru}(\text{III})/\text{Ru}(\text{II})$ redox potentials and thus allow to generate a family of catalysts with a controlled reactivity.⁴ In addition to the electronic effects, examples also exist where sterically hindered ligands strongly influence the reactivity of a $\text{Ru}=\text{O}$ system with regard to substrate oxidation.⁵

Oxazoline-containing ligands have been shown to be a convenient choice because of their easy synthetic accessibility, modular nature, and applicability in a wide range of metal-catalyzed transformations.^{6–8} Recently, we have reported a family of new Ru complexes containing tridentate and oxazolinic ligands together with the preliminary studies of their epoxidation catalytic activity.⁹ Our results have shown that the reactivity of the $\text{Ru}-\text{OH}_2$ complexes is practically independent of the redox potentials of the catalyst but that it is strongly dependent on the geometry of the tridentate ligands (meridional, trpy, or facial, tpm). Given these results, we have now focused our attention on the oxazolinic ligand with the aim of studying the influence of its substituents on the catalytic performance of the complexes.

In the present paper we report the synthesis, structure, spectroscopy, and redox properties of new Ru complexes containing neutral and anionic oxazolinic ligands, iPr-box-C and iPr-box-O, together with the facial tridentate tpm ligand, Chart 1. The catalytic performance of this family of complexes has been tested with regard to the epoxidation of alkenes and is reported here together with the activity of other oxazolinic complexes previously synthesized in our group for purposes of comparison. The predictions based on computed energy barriers agree with the distinctive catalytic results experimentally found for two catalysts that bear different substituents (isopropyl or benzyl) at the oxazole ring.

EXPERIMENTAL SECTION

Materials. All reagents used in the present work were obtained from Aldrich Chemical Co and were used without further purification. Reagent grade organic solvents were obtained from SDS, and high purity deionized water was obtained by passing distilled water through a nanopure

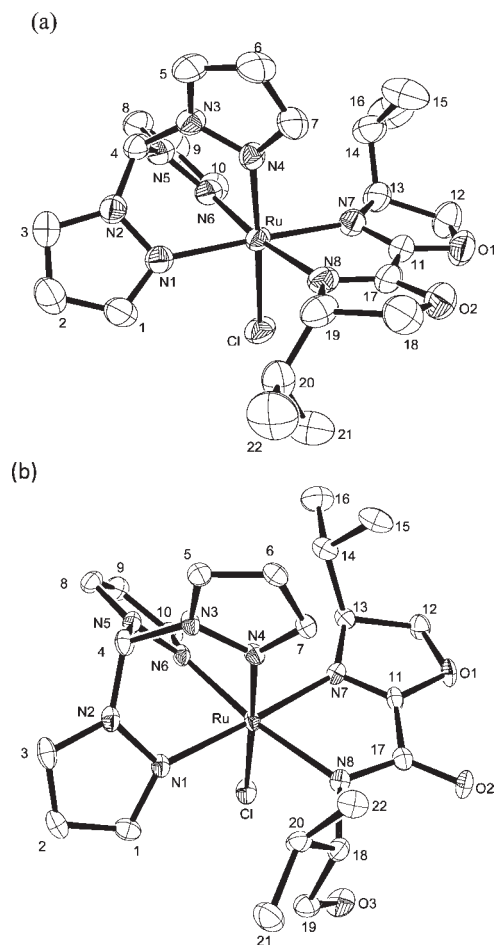


Figure 1. ORTEP view (ellipsoids are drawn at 50% probability level) of the molecular structure of cation **2c** (a) and neutral complex **2o** (b) including the atom numbering scheme.

Mili-Q water purification system. $\text{RuCl}_3 \cdot 2\text{H}_2\text{O}$, was supplied by Johnson and Matthey Ltd. and was used as received.

Preparations. Ligands (see Chart 1) iPr-box-C ((4*S*,4'*S*)-(–)-4,4',5,5'-tetrahydro-4,4'-bis(1-methylethyl)-2,2'-bioxazole)¹⁰ and tpm (tris-pyrazolylmethane)¹¹ as well as the complexes **1**¹² and **3'**c/**3'o**⁹ were prepared as described in the literature. All synthetic manipulations were routinely performed under nitrogen atmosphere using Schlenk tubes and vacuum line techniques. Electrochemical experiments were performed under either N_2 or Ar atmosphere with degassed solvents.

$[\text{Ru}^{\text{II}}\text{Cl}(\text{iPr-box-C})(\text{tpm})](\text{BF}_4) \cdot 1.7(\text{CH}_3\text{CH}_2)_2\text{O}$, **2c** · $1.7(\text{CH}_3\text{CH}_2)_2\text{O}$, and $[\text{Ru}^{\text{II}}\text{Cl}(\text{iPr-box-O})(\text{tpm})] \cdot 2.5\text{CH}_3\text{OH}$, **2o** · $2.5\text{CH}_3\text{OH}$. A sample of **1** (100 mg, 0.24 mmol) was added to a 100 mL round bottomed flask containing a degassed solution of LiCl (20 mg, 0.47 mmol) in $\text{EtOH}:\text{H}_2\text{O}$ 3:1 (40 mL), under magnetic stirring. Then, NEt_3 (0.07 mL) was added, and the reaction mixture was stirred at room temperature (RT) for 30 min. At this point, iPr-box-C (53 mg, 0.24 mmol) was added, and the mixture was then heated at reflux for 5 h. The hot solution was filtered off in a frit, and the volume was reduced to dryness in a rotary evaporator. The solid obtained was then dissolved in CH_2Cl_2 and washed several times with water. The organic phase was then dried over MgSO_4 , and the mixture again reduced to dryness. The solid obtained in this manner was a mixture of chloro complexes **2c** and **2o** that were separated by column chromatography (alumina; $\text{CH}_2\text{Cl}_2/\text{MeOH}$ 95:5). Complex **2c** was dissolved in MeOH (10 mL), and a saturated aqueous solution of NaBF_4 (1.5 mL) was added. The red solid obtained was filtered off in a frit and recrystallized from a hot mixture of

$\text{CH}_2\text{Cl}_2/\text{ether}$ (1:1). Chloro complex **2o** was recrystallized in methanol-diethylether solution. For **2c**, yield: 45 mg (24%). Anal. Found (Calcd.) for $\text{C}_{22}\text{H}_{30}\text{N}_8\text{O}_2\text{ClRuBF}_4 \cdot 1.7\text{C}_4\text{H}_{10}\text{O}$: C, 43.91(43.91), N, 13.88 (14.22), H, 5.62 (6.01). IR: $\nu = 1503\text{ cm}^{-1}$ (CN). ^1H NMR (CDCl_3 , 500 MHz, 298 K): δ 9.64 (H4, s), 8.63 (H5, d, 2.4 Hz), 8.51 (H3, d, 2.4 Hz), 8.47 (H8, d, 2.4 Hz), 8.22 (H1, d, 1.9 Hz), 8.20 (H10, d, 1.9 Hz), 7.13 (H7, d, 1.7 Hz), 6.50 (H2, H9, m), 6.46 (H6, t, 2.5 Hz), 4.98 (H12b, t, 9.5 Hz), 4.89 (H18, d, 8.6 Hz), 4.86 (H12a, dd, 6.2 and 9.5 Hz), 4.53 (H13, dddd, 2.7, 6.2, and 9.5 Hz), 4.21 (H19, dt, 9.0 and 3.4 Hz), 2.45 (H20, m), 1.23 (H14, m), 1.17 (H21, d, 6.6 Hz), 0.94 (H22, d, 7.1 Hz), 0.73 (H15, d, 7.6 Hz), 0.46 (H16, d, 6.9 Hz). ^{13}C NMR (CDCl_3 , 500 MHz, 298 K): δ 158.6 ppm (C11, C17), 148.4 (C1), 146.8 (C10), 143.9 (C7), 135.4 (C5), 134.6 (C3, C8), 108.9 (C2, C9), 108.5 (C6), 75.4 (C4), 72.9 (C12), 72.2 (C18), 71.1 (C19), 69.9 (C13), 28.6 (C20), 19.0 (C14), 18.9 (C22), 18.7 (C15), 14.5 (C21), 14.4 (C16). $E_{1/2}$ (CH_2Cl_2) = 0.79 V vs SSCE. UV-vis (CH_2Cl_2): λ_{max} , nm (ϵ , $\text{M}^{-1}\text{ cm}^{-1}$) 2922 (89216), 326 (sh 6505), 464 (5204). For **2o**, yield: 43 mg (31%). Anal. Found (Calcd.) for $\text{C}_{22}\text{H}_{31}\text{N}_8\text{O}_3\text{ClRu} \cdot 2.5\text{CH}_3\text{OH}$: C, 43.78 (43.83), N, 16.67 (16.65), H, 6.15 (6.44). IR: $\nu = 1568\text{ cm}^{-1}$ (CN). $E_{1/2}$ (CH_2Cl_2) = 0.22 V vs SSCE. UV-vis (CH_2Cl_2): λ_{max} , nm (ϵ , $\text{M}^{-1}\text{ cm}^{-1}$) 285 (8400), 312 (7350), 413 (sh, 4500).

For the NMR assignment we used the same numbering scheme as that for the X-ray structures displayed in Figure 1.

[Ru^{II}(iPr-box-C)(tpm)OH₂](PF₆)₂ · 0.8H₂O, **3c · 0.8H₂O.** A sample of AgPF_6 (16.9 mg, 0.067 mmol) was added to a solution of acetone: H_2O 1:2 (20 mL) containing **2c** (40 mg, 0.051 mmol), and the mixture was heated at reflux for 1.5 h. The precipitate of AgCl formed was filtered off through a frit containing Celite, and the volume reduced in a rotary evaporator under reduced pressure until a brown precipitate appeared. The solid obtained was filtered through a frit, washed with cold water, and dried with ether. Yield: 41.6 mg (95%). Anal. Found (Calcd.) for $\text{C}_{22}\text{H}_{32}\text{N}_8\text{O}_3\text{RuP}_2\text{F}_{12} \cdot 0.8\text{H}_2\text{O}$: C, 31.02 (30.66), N, 12.79 (13.00), H, 4.22 (3.93). IR: $\nu = 1507\text{ cm}^{-1}$ (CN). ^1H -NMR (d_6 -acetone, 600 MHz, 298 K): δ 9.67 (H4, s), 8.67 (H5, d, 2.8 Hz), 8.58 (H3, d, 2.1 Hz), 8.51 (H8, d, 1.9 Hz), 8.44 (H1, d, 1.9 Hz), 8.14 (H10, d, 1.9 Hz), 6.81 (H7, t, 2.5 Hz), 6.78 (H2, H9, m), 6.63 (H6, t, 2.5 Hz), 5.50 (H2O), 5.20–5.12 (H12b, H18, H12a, m), 4.87 (H13, m), 4.3 (H19, m), 2.55 (H20, m), 1.20 (H14, m), 1.07 (H21, d, 6.7 Hz), 0.99 (H22, d, 7.6 Hz), 0.73 (H15, d, 7.0 Hz), 0.53 (H16, d, 7.0 Hz). $E_{1/2}$ (phosphate buffer pH = 7) = 0.38 V vs SSCE. UV-vis (phosphate buffer pH = 7): λ_{max} , nm (ϵ , $\text{M}^{-1}\text{ cm}^{-1}$) 275 (1863), 308 (sh, 1517), 421 (1327). UV-vis (CH_2Cl_2): λ_{max} , nm (ϵ , $\text{M}^{-1}\text{ cm}^{-1}$) 277 (9810), 311 (8049), 417 (7070).

[Ru^{II}(iPr-box-O)(tpm)OH₂](PF₆) · 1.1H₂O, **3o · 1.1H₂O.** A sample of AgPF_6 (23.8 mg, 0.094 mmol) was added to 15 mL of H_2O containing **2o** (49 mg, 0.073 mmol) and a few crystals of ascorbic acid, and the mixture was heated at reflux for 3 h under N_2 atmosphere. AgCl was filtered off through a frit containing Celite, and the volume reduced in a rotary evaporator until the appearance of a yellow precipitate. The solid obtained was filtered and washed with diethylether. Yield: 38.2 mg (71%). Anal. Found (Calcd.) for $\text{C}_{22}\text{H}_{33}\text{N}_8\text{O}_4\text{Ru} \cdot 1.1\text{H}_2\text{O}$: C, 30.19 (29.88), N, 12.51 (12.67), H, 4.22 (4.01). IR: $\nu = 1590\text{ cm}^{-1}$ (CN). ^1H NMR (d_6 -acetone, 600 MHz, 298 K): δ 9.62 (H4, s), 8.62 (H5, d, 2.8 Hz), 8.59 (H8, d, 2.8 Hz), 8.54 (H3, d, 2.3 Hz), 8.47 (H7, d, 2.3 Hz), 8.24 (H10, d, 2.8 Hz), 7.86 (H1, d, 2.3 Hz), 6.74 (H6, t, 2.5 Hz), 6.69 (H9, t, 2.5 Hz), 6.62 (H2, t, 2.5 Hz), 4.83 (H12, broad s), 4.64 (H13, ddd, 3.3, 7.6, and 8.8 Hz), 1.50 (H14, m), 0.73 (H15, d, 7.2 Hz), 0.60 (H16, d, 6.4 Hz). $E_{1/2}$ (phosphate buffer pH = 7) = 0.22 V vs SSCE. UV-vis (phosphate buffer pH = 7): λ_{max} , nm (ϵ , $\text{M}^{-1}\text{ cm}^{-1}$) 289 (1947), 323 (2033), 400 (sh).

Instrumentation and Measurements. IR spectra were recorded on a Mattson Satellite FT-IR using a MKII Golden Gate Single Reflection ATR System. UV-vis spectroscopy was performed in a Cary 50 Scan (Varian) UV-vis spectrophotometer with 1 cm quartz cells. pH measurements were done using a Micro-pH-2000 from Crison. Cyclic voltammetry (CV) experiments were performed in a JI-Cambria

Table 1. Crystal Data for Complexes **2c and **2o****

	2c	2o
empirical formula	$\text{C}_{22}\text{H}_{30}\text{N}_8\text{O}_2\text{ClRuBF}_4$	$\text{C}_{25}\text{H}_{39}\text{N}_8\text{O}_5\text{ClRu}$
Fw	661.87	668.16
cryst system	monoclinic	monoclinic
space group	$P2_1$	$P2_1$
<i>a</i> , Å	7.497(2)	7.7404(18)
<i>b</i> , Å	16.765(5)	17.076(4)
<i>c</i> , Å	11.495(4)	11.628(3)
α , deg	90	90
β , deg	90.351(5)	97.103(4)
γ , deg	90	90
<i>V</i> , Å ³	1444.6(8)	1525.2(6)
formula units/cell	2	2
temp, K	300(2)	100(2)
$\lambda(\text{Mo-K}\alpha)$, Å	0.71073	0.71073
ρ_{calc} , g cm ⁻³	1.522	1.455
R_1^a	0.0287	0.0374
wR_2^b	0.0719	0.0741

^a $R_1 = \sum ||F_o| - |F_c|| / \sum |F_o|$. ^b $wR_2 = [\sum w(F_o^2 - F_c^2)^2 / \sum w(F_o^2)^2]^{1/2}$, where $w = 1 / [\sigma^2(F_o^2) + (0.0377P)^2 + 1.65P]$ and $P = (F_o^2 + 2F_c^2) / 3$.

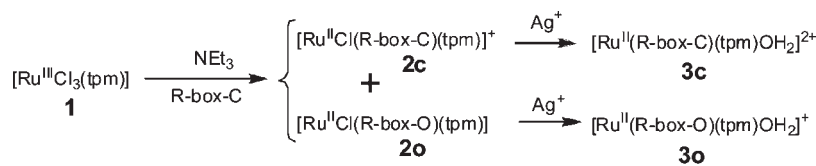
ICH-660 potentiostat using a three electrode cell. Glassy carbon disk electrodes (3 mm diameter) from BAS were used as working electrodes, platinum wire as auxiliary, and SSCE as the reference electrode. All cyclic voltammograms presented in this work were recorded at a 100 mV/s scan rate under nitrogen atmosphere. The complexes were dissolved in previously degassed solvents containing the necessary amount of supporting electrolyte to yield a 0.1 M ionic strength solution. In dichloromethane, (*n*-Bu₄N)(PF₆), TBAH, was used as supporting electrolyte. In aqueous solutions the pH was adjusted from 0 to 2 with HCl, and potassium chloride was added to keep a minimum ionic strength of 0.1 M. From pH 2–10, 0.1 M phosphate buffers were used, and from pH 10–12 diluted, CO₂ free, NaOH. All $E_{1/2}$ values reported in this work were estimated from cyclic voltammetry as the average of the oxidative and reductive peak potentials ($E_{p,a} + E_{p,c}$)/2. Unless explicitly mentioned the concentration of the complexes was approximately 1 mM.

NMR experiments were carried out on Bruker 500MHz and 600MHz spectrometers. Samples were run in d_6 -acetone or CDCl_3 , and spectra were calibrated using the residual solvent and/or tetramethylsilane signals. Elemental analyses were performed using a CHNS-O Elemental Analyzer EA-1108 from Fisons.

Catalytic Oxidation Experiments. Catalytic essays have been performed in dichloromethane dried over CaH_2 at room temperature (RT). In a typical run, ruthenium catalyst (0.002 mmol), alkene (0.2 mmol), and $\text{PhI}(\text{OAc})_2$ (0.4 mmol) were stirred at RT in dichloromethane (2.5 mL) for 24 h. The end of the reaction was indicated by the disappearance of solid co-oxidant. After addition of an internal standard, an aliquot was taken for GC analysis. The oxidized products were analyzed in a Shimadzu GC-2010 gas chromatography apparatus equipped with an Astec CHIRALDEX G-TA Column (10 m × 0.25 mm diameter) incorporating a FID detector. GC conditions: initial temperature 80 °C for 10 min, ramp rate 10°/min, final temperature 170 °C, injection temperature 220 °C, detector temperature 250 °C. All catalytic oxidations were carried out under nitrogen atmosphere.

X-ray Structure Determinations. Suitable crystals of **2c** and **2o** were grown by slow diffusion of ether into a MeOH solution as dark red needles or plates.

Scheme 1. Synthetic Pathways and Labeling Scheme for Complexes Described in This Work



R= iPr; when R= Bz, analogous **2'c**, **2'o**, **3'ca**, and **3'o** complexes are obtained

Data Collection. Intensity data for **2o** and **2c** were collected at 100 and 300 K respectively on a BRUKER SMART APEX CCD diffractometer using graphite-monochromated Mo $K\alpha$ radiation from an X-ray Tube. Full-sphere data collection was carried out with ω and φ scans.

Structure Solution and Refinement. The structure was solved by direct methods and refined by full-matrix least-squares methods on F^2 using the Shelxs-97 and Shelxl-97 softwares, respectively. The non-hydrogen atoms were refined anisotropically. The H-atoms were placed in geometrically optimized positions and forced to ride on the atom to which they were attached, except for the water molecule H atoms of **2o** which were placed on the difference electron density map and refined with an antibumping restraint of 1.50(1) Å.

The crystallographic data as well as details of the structure solution and refinement procedures are reported in Table 1. CCDC 827784 and 827785 contain the supplementary crystallographic data for this paper. These data can be obtained free of charge from the Cambridge Crystallographic Data Centre via www.ccdc.cam.ac.uk/conts/retrieving.html.

Computational Details. The density functional calculations were performed on all the systems at the GGA level with the Gaussian09 set of programs.¹³ The density functional theory (DFT) calculations were carried out with the functional BP86 with the gradient corrections taken from the work of Becke and Perdew.¹⁴ The electronic configuration of the molecular systems was described by the standard SVP basis set, that is, the split-valence basis set with polarization functions of Ahlrichs and co-workers, for H, C, N, and O.¹⁵ For Ru we used the small-core, quasi-relativistic Stuttgart/Dresden effective core potential (standard SDD basis set in Gaussian 09) basis set, with an associated (8s7p6d)/[6s5p3d] valence basis set contracted according to a (311111/22111/411) scheme.¹⁶

The geometry optimizations were performed without symmetry constraints, and the nature of the extrema was checked by analytical frequency calculations. Furthermore, all the extrema were confirmed by calculation of the intrinsic reaction paths. The energies reported in this work are Gibbs energies computed at 298 K in gas phase including solvent effects. These latter effects were estimated in single point calculations on the gas-phase optimized structures using the polarizable continuous solvation (PCM) method and considering H₂O as the solvent.¹⁷

Calculations of the local Fukui functions were also performed. The Fukui function¹⁸ is a reactivity index that connects the concepts of the Fukui frontier orbitals with DFT. It was defined by Yang and Parr as the partial derivative of the electron density with respect to the total number of electrons with constant external potential or as the derivative of the chemical potential with respect to the external potential keeping constant the total number of electrons of the system:

$$f(\vec{r}) = \left(\frac{\delta\mu}{\delta v(\vec{r})} \right)_N = \left(\frac{\partial\rho(\vec{r})}{\partial N} \right)_{v(\vec{r})} \quad (1)$$

Over the past years, Fukui functions have been used to explain the regioselectivity in chemical reactions.¹⁹ The Fukui function describes the local changes in the electronic density of a system due to a perturbation in the total number of electrons. For a molecule or an atom, the

derivative of the eq 1 is not continuous with the number of electrons and difficult to evaluate.²⁰ So, Parr and Yang¹⁸ defined the Fukui functions: $f^+(r)$ and $f^-(r)$ corresponding to the reactivity indexes that describe the attack toward our system by a nucleophilic or electrophilic species, where the superscripts + and – refer to the derivatives of the right and left of the central part, respectively.

By applying the finite-difference approximation it is easily shown that the Fukui functions can be obtained from density differences. If these functions are condensed to the specific atomic regions of the three-dimensional (3D) molecular space we obtain the condensed Fukui functions:

$$f_x^+ = q_x(N+1) - q_x(N) \quad (2)$$

$$f_x^- = q_x(N) - q_x(N-1) \quad (3)$$

where the parameters q_x are the charges of the atom X calculated in the systems with N , $N-1$, and $N+1$ electrons keeping the optimized geometry of the molecule with N electrons. In this work, we have used charges derived from Natural Population Analysis (NPA) to calculate the condensed Fukui functions.²¹

RESULTS AND DISCUSSION

Synthesis and Solid State Structure. The synthetic strategy followed for the preparation of the complexes described in the present paper is outlined in Scheme 1.

The trichloro Ru complex $[\text{Ru}^{\text{III}}\text{Cl}_3(\text{tpm})]$, **1**, is used as starting material, followed by reduction with NEt₃ in the presence of the bisoxazolinic ligand, iPr-box-C, to form the corresponding monochloro Ru(II) complex **2c**. However, the reaction leads to a mixture of two complexes: the expected **2c** and a second chloro complex, **2o**, where the oxazolinic ligand has suffered a nucleophilic attack by an OH[–] group, leading to ring cleavage and thus generating the new anionic unsymmetric oxazolinic-amidate ligand iPr-box-O[–] (see Chart 1). This ring-opening is attributed to a Ru-assisted process once the oxazoline ligand is coordinated, because of an enhancement of the iminic C atom electrophilicity upon coordination as has previously been described by our group.⁹ These Ru–Cl complexes are easily separated by column chromatography since **2c** is cationic whereas **2o** is a neutral complex. The corresponding Ru–OH₂ complexes **3** are easily obtained from the corresponding Ru–Cl complexes in the presence of stoichiometric amounts of Ag⁺. The X-ray diffraction structures for both chloro complexes have been resolved, and the corresponding crystallographic data and selected bond distances and angles are reported in Table 1 and Supporting Information, Table S1. ORTEP views together with their labeling schemes are depicted in Figure 1.

In all cases, the Ru metal center adopts an octahedrally distorted type of coordination where the tpm ligand is bonded in a facial manner and the iPr-box-C and the iPr-box-O[–] oxazoline ligands act in a didentate fashion. The facial topology of the tpm

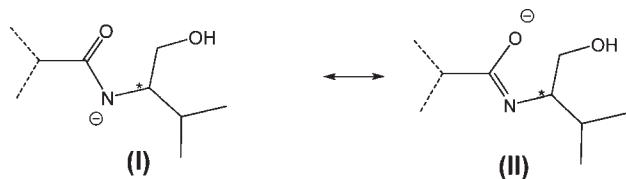
Table 2. UV–vis Spectroscopic Features in CH₂Cl₂ for the Ru–Cl Complexes and in Aqueous Solution for the Ru–Aquo Complexes

compound	assignment	λ_{max} , nm (ϵ , M ⁻¹ cm ⁻¹)
[Ru ^{II} Cl(Bz-box-C)(tpm)](BF ₄), 2'c ^a	$\pi \rightarrow \pi^*$	271 (9900), 326 (7200)
	$d\pi \rightarrow \pi^*$	468 (6400)
[Ru ^{II} Cl(Bz-box-O)(tpm)], 2'o ^a	$\pi \rightarrow \pi^*$	270 (6900), 335 (sh)
	$d\pi \rightarrow \pi^*$	388 (8600)
[Ru ^{II} Cl(iPr-box-C)(tpm)](BF ₄), 2c	$\pi \rightarrow \pi^*$	292 (8916), 326 (sh, 6505)
	$d\pi \rightarrow \pi^*$	464 (5204)
[Ru ^{II} Cl(iPr-box-O)(tpm)], 2o	$\pi \rightarrow \pi^*$	285 (8400), 312 (7350)
	$d\pi \rightarrow \pi^*$	413 (sh, 4500)
[Ru ^{II} (Bz-box-C)(tpm)OH ₂](BF ₄) ₂ , 3'c ^a	$\pi \rightarrow \pi^*$	263 (9800), 310 (sh),
	$d\pi \rightarrow \pi^*$	423 (4150)
[Ru ^{II} (Bz-box-O)(tpm)OH ₂](BF ₄) ₂ , 3'o ^a	$\pi \rightarrow \pi^*$	260 (6210), 330 (5250)
	$d\pi \rightarrow \pi^*$	387 (sh)
[Ru ^{II} (iPr-box-C)(tpm)OH ₂](BF ₄) ₂ , 3c	$\pi \rightarrow \pi^*$	275 (1863), 308 (sh, 1517)
	$d\pi \rightarrow \pi^*$	421 (1327)
[Ru ^{II} (iPr-box-O)(tpm)OH ₂](BF ₄) ₂ , 3o	$\pi \rightarrow \pi^*$	289 (1947), 323 (2033)
	$d\pi \rightarrow \pi^*$	400 (sh)

^a Reference 9.

ligand forces that in both cases the chloride ligand coordinates *cis* to the oxazoline ligands. All bond distances and angles are within the expected values for this type of complexes.²² The 3D arrangement of molecules in complex **2c** displays a network of intermolecular H-bonding interactions (with interatomic distances below 2.75 Å, see Supporting Information) involving the chloride ligand as well as the PF₆⁻ counterions of the structure. The close contact of each Cl ligand with a tpm H atom of the neighboring molecule allows the establishment of one-dimensional (1D) chains in the *a* axis direction that are joined together through the PF₆⁻ anions.

The X-ray structure of complex **2o** presents C17–O2 and C17–N8 bond distances (see Figure 1b) of 1.266 and 1.320 Å, respectively, that are consistent with an intermediate situation between the two resonant forms of the amidate ligand,⁹ therefore pointing to a charge delocalization through the NCO backbone:



Spectroscopic Properties. The combination of 1D and 2D NMR spectra, registered in d₆-acetone or CDCl₃, allows to unambiguously identify the resonances of all the protons for complexes **2c** and **3c**. The NMR assignment is described in the Experimental Section and is consistent with the structures found in the solid state as expected for a Ru(II) d⁶ type of ion. However, for complexes **2o** and **3o** some of the expected resonances either appear as wide signals or are missing because of dynamic effects arising from the open oxazole ring in the iPr-box-O ligand. In

solution, none of the complexes described in this paper possesses any symmetry element so all the resonances of the ligands are expected to be different as confirmed experimentally. The complete 1D and 2D NMR characterization of complexes **2c**, **2o**, **3c**, and **3o** is presented in the Supporting Information.

In the case of Ru–H₂O complex **3c**, the ¹H NMR spectrum registered in d₆-acetone (Supporting Information) shows a splitting of the signals which is consistent with the presence of two different species. A study on the evolution of the resonances with time reveals the presence of a main species corresponding to the aqua complex **3c** together with a new complex, resulting from the substitution of aqua by acetone coming from the solvent.

The UV–vis spectra of all complexes are displayed in the Supporting Information whereas their main features are presented in Table 2 together with other similar complexes recently described by our group.⁹

The complexes exhibit ligand based $\pi \rightarrow \pi^*$ bands below 350 nm and relatively intense bands above 350 nm assigned mainly to $d\pi \rightarrow \pi^*$ MLCT transitions. For the Ru–Cl complexes the MLCT bands are shifted to the red with regard to the analogous Ru–OH₂ species because of the relative destabilization of the $d\pi(\text{Ru})$ levels provoked by the chloro ligand. In particular, the replacement of the Cl ligand by aqua (**3c** vs **2c** or **3o** vs **2o**) produces a blue shift of roughly 13–43 nm. The replacement of benzyl by isopropyl groups in the oxazolinic ligand does not reveal any important change in the bands of the UV–vis spectra for the complexes having the closed ligands (**2c** vs **2'c** or **3c** vs **3'c**), but a slight bathochromic shift is observed for complexes containing the iPr-box-O ligand (**2o** and **3o**) with regard to the analogous with Bz-box-O (**2'o** and **3'o**), which is in accordance with the higher electron-donor character of the iPr substituent when compared to Bz. This indicates that the opening of the oxazole ring seemingly allows a more effective transmission of the electron density from the oxazoline substituents to the metal center in Ru(II) species.

Redox Properties. The redox properties of the Ru–Cl and Ru–aqua complexes described in the present work were investigated by means of CV techniques. All cyclic voltammograms are shown in the Supporting Information, Figure S7.

The cyclic voltammograms of chloro complexes **2c** and **2o**, registered in CH₂Cl₂+0.1 M TBAP, exhibit chemically reversible waves assigned to the corresponding Ru(III/II) couples. For complex **2c** this wave appears at $E_{1/2} = 0.79$ V vs SSCE, whereas for the complex **2o** this wave is cathodically shifted to $E_{1/2} = 0.22$ V, as expected from the higher electron-donating capacity of the anionic iPr-box-O⁻ ligand with regard to the neutral iPr-box-C. If we compare these redox potentials with those corresponding to the analogous chloro complexes having the Bz-Box-C and Bz-Box-O oxazolinic ligands, **2'c** ($E_{1/2} = 0.83$ V) and **2'o** ($E_{1/2} = 0.24$ V), we can see that complexes **2c** and **2o** display a slight cathodic shift of 40 and 20 mV respectively because of the stronger electron-withdrawing capacity of the benzyl groups with regard to the iPr groups. It is interesting to note that the distinctive electronic effects of the iPr/Bz substituents were manifested in the UV–vis spectra only for complexes containing the open R-box-O ligands thus indicating that oxidation of the Ru metal center may enhance the electronic influence exerted by the substituents of the closed R-box-C ligands.

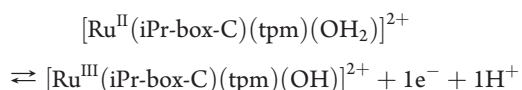
The redox potentials for the Ru–aqua complexes **3c** and **3o** are summarized in Table 3 together with other relevant Ru–aqua complexes previously described in the literature for purposes of comparison.^{9,23,24}

Table 3. pK_a and Electrochemical Data (pH = 7) for the Aquocomplexes Described in This Work and Others for Purposes of Comparison

entry	complex ^a (T)(D)Ru–OH ₂	E _{1/2} ^b (III/II)	E _{1/2} ^b (IV/III)	ΔE ^c	pK _a (II)	pK _a (III)	ref
1	tpm-bpy	0.40	0.71	310	10.8	1.9	23a
2	tpm-Bz-box-C, 3' <i>c</i>	0.38			>10	1.8	9
3	tpm-Bz-box-O, 3' <i>o</i>	0.17	0.37	200	11.0	3.9	9
4	3 <i>c</i>	0.38			>12	1.8	^d
5	3 <i>o</i>	0.16			10.5	2.3	^d
6	trpy-bpy	0.49	0.62	130	9.7	1.7	23b
7	trans-trpy-pic	0.21	0.45	240	10	2	12
8	cis-trpy-pic	0.38	0.56	180	10	3.7	12
9	trpy-acac	0.19	0.56	370	11.2	5.2	24a

^aT stands for tridentate ligand whereas D for didentate; acac = acetylacetonate, pic = picolinate. ^bRedox potentials in volts are reported with regard to the SSCE reference electrode. ^cΔE = E_{1/2}(IV/III) – E_{1/2}(III/II) in mV. ^dThis work.

The aquocomplexes' redox potentials are pH dependent because of the capacity of the mentioned aqua ligand to lose protons. This ability to release H⁺ is also responsible for the easy accessibility of Ru higher oxidation states as shown in the following equation as an example,



The complete thermodynamic information regarding the Ru-aqua type of complex can be extracted from the Pourbaix diagrams, exhibited in Figure 2 for 3*c* and 3*o*.

For complex 3*c* the absence of information in the Pourbaix diagram above pH = 12 is presumably because at this high pH the hydrolysis of the oxazolinic iPr-box-C ligand is taking place.⁹ The pK_a values for the Ru^{II}–OH₂ and Ru^{III}–OH₂ species, gathered in Table 3, can be calculated from the slope breaks of the Ru^{III}/Ru^{II} couple.

A careful study of Table 3 allows extracting the following conclusions: (a) as shown in entries 1, 2, and 4, the replacement of a bpy by a Bz-box-C or iPr-box-C ligand produces a decrease of 20 mV of the Ru(III/II) redox couple because of the lower electron-withdrawing capacity of the oxazolinic ligand vs the bpy ligand. A similar effect is observed when comparing similar complexes but replacing trpy by tpm as for instance in entries 1 and 6; (b) entries 4 and 5 show the cathodic shift of 220 mV produced by the replacement of a neutral oxazolinic ligand with the corresponding hydrolyzed anionic ligand because of stabilization of Ru(III), as was the case for the previously described complexes 3'*c* and 3'*o* (entries 2 and 3). This behavior is also found when comparing Ru-trpy-bpy (entry 6) with the analogous picolinate and acetylacetonate complexes (entries 7–9); (c) the replacement of a benzyl substituent by iPr does not produce any change in the Ru(III/II) couple of complexes 3*c* and 3'*c* and only a slight variation of 10 mV in the case of complexes 3*o* and 3'*o*, then suggesting that for aquocomplexes the redox behavior is predominantly governed by the protonation/deprotonation processes at the aquo ligand; (d) In all cases, the exchange of an anionic ligand by a neutral ligand slightly affects pK_{a,II} but strongly influences pK_{a,III}. This can be interpreted in the sense

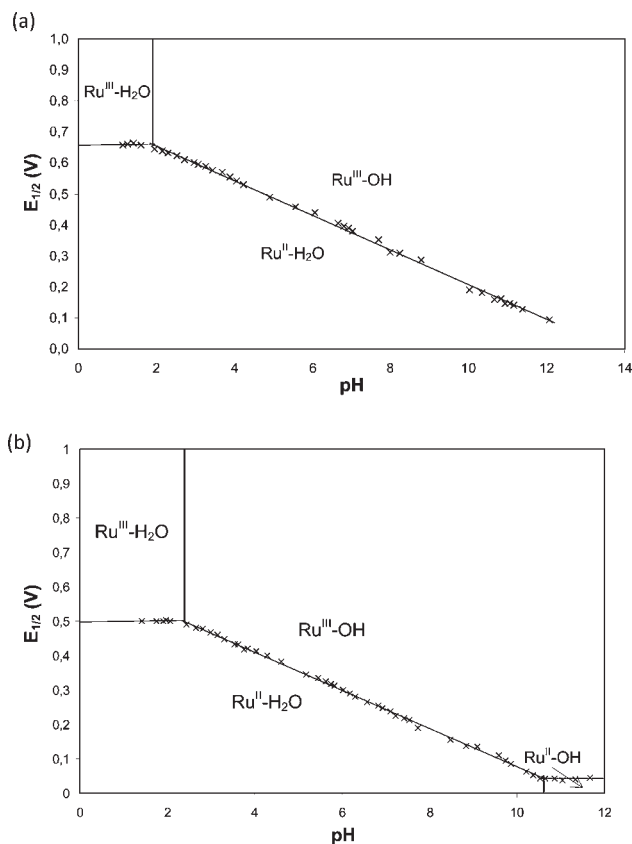


Figure 2. E_{1/2} vs pH or Pourbaix diagram of complexes 3*c* (a) and 3*o* (b). The pH-potential regions of stability for the various oxidation states and their dominant proton compositions are indicated.

that the higher the oxidation state, the stronger the σ donation capability provided by the anionic ligand.

Catalytic Epoxidations. The catalytic activity of the ruthenium complexes 3*c* and 3*o* together with other aquocomplexes previously synthesized in our group, 3'*c* and 3'*o*, was investigated in the epoxidation of different alkenes given the interest of the epoxidation reaction in both bulk and fine chemistry that use epoxides as starting materials for a variety of reactions.²⁵

Initial assays were performed with *trans*-stilbene as test substrate using the following conditions: CH₂Cl₂ as solvent; PhI(OAc)₂ as oxidant; catalyst:substrate:oxidant molar ratio of 1:100:200. The results obtained are gathered in Table 4 together with other Ru-oxazoline complexes for purposes of comparison.⁹ No epoxidation occurred in the absence of catalyst in any case.

A first glance at Table 4 shows that in all the cases the main product formed is *trans*-stilbene oxide (TSO) with minor amounts of benzaldehyde (BzA) and that the catalysts bearing the closed oxazolinic rings are in general more active than those containing the open rings. Also, catalysts bearing the facial tpm ligand (entries 1–5) are markedly more active than those containing the meridional trpy (entries 6 and 7). The difference between pairs of analogous complexes with open/closed ligands is specially pronounced when comparing complexes 3'*c* and 3'*o* (entries 1 and 2), and this effect has already been explained⁹ as a consequence of π-stacking effects between the substrate and the CH₂Ph substituents of the Bz-box-C ligand. This kind of interactions can only take place in the case of catalyst 3'*c* given the high mobility of the benzyl arm in the hydrolyzed ring of 3'*o* that

leads to a clearly better performance for the former. However, for the case of the analogous complexes **3c** and **3o**, where π -stacking cannot occur, a rather small difference in reactivity is observed (entries 3 and 5). Finally we can perceive that, under dark conditions (entry 4), catalyst **3c** is slightly more active in the epoxidation of *trans*-stilbene leading also to the best epoxide/benzaldehyde ratio. To the best of our knowledge our Ru-oxazoline complexes are among the most selective ruthenium catalysts described in the literature for the oxidation of *trans*-stilbene,^{26,27} even though the experimental conditions are not identical to those reported previously.

With the aim to investigate the influence of the different substituents at the oxazolinic ligands in the reactivity of ruthenium complexes, we decided to test **3'c** and **3c** in the epoxidation of *cis*- β -methylstyrene and 4-vinylcyclohexene under the same experimental conditions. The results are gathered in Table 5, where the main product formed is the corresponding epoxide with minor amounts of other oxidation products such as benzaldehyde.

Both complexes display a good performance and selectivity except for the epoxidation of 4-vinylcyclohexene with complex **3c**, where a moderate activity is obtained. The selectivity for the epoxide in the oxidation of *cis*- β -methylstyrene is moderate in both cases, but it is remarkable that only the *cis* epoxide is

Table 4. Catalytic Oxidation of *trans*-Stilbene by Ru-Aqua Complexes Using $\text{PhI}(\text{OAc})_2$ as Oxidant^a

entry	cat	conversion, %	selectivity, % ^b	ratio epoxide/benzaldehyde ^c
1	3'c	68.9	89	3.9
2	3'o	34.5	96	12.3
3	3c	55.2	85	19.6
4	3c^d	62.5	87	22.6
5	3o	51.2	81	17.7
6	trpy-Bz-box-C^e	16.3	82	2.4
7	trpy-Bz-box-O^e	15.5	81	2.1

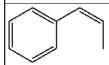
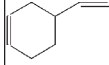
^a Reaction conditions: catalytic oxidations were performed by dissolving the Ru-aqua complex (0.002 mmol) in degassed dichloromethane (2.5 mL) containing *trans*-stilbene (0.2 mmol) and $\text{PhI}(\text{OAc})_2$ (0.4 mmol). The reaction mixture was stirred at RT for 24 h. After addition of an internal standard, an aliquot was taken for GC analysis. ^b Selectivity for epoxide, [yield/conversion] \times 100. ^c Assuming that two molecules of benzaldehyde come from the scission of a single stilbene molecule. ^d In the dark. ^e Ref 9.

produced, with no traces for the isomerization toward the *trans* diastereoisomer. This is in agreement with either a potential O-atom transfer concerted mechanism or a stepwise mechanism with a short life intermediate having a half-time smaller than the time required for the rotation of the attacked C–C bond.²⁸ Similar results had been observed with several ruthenium complexes with nitrogen-donor ligands.^{27b,29}

For 4-vinylcyclohexene, complex **3'c** leads to good conversions and a very high regioselectivity for oxidation of the substrate at the alkene ring position whereas complex **3c** has been shown to be regioselective for the oxidation of the terminal vinyl position, with a moderate conversion. To the best of our knowledge, the selective epoxidation at the terminal position of this substrate has never been reported with ruthenium aqua complexes, although regioselective catalysts for alkene carbon–carbon bond cleavage to form aldehydes with significant preference for primary alkenes have been described.³⁰ The different behavior shown by the two catalysts cannot be explained in terms of steric hindrance since complex **3'c**, having a benzyl substituent at the box-C ligand, should in advance exhibit a certain preference for the less hindered terminal alkene. Thermodynamic effects arising from the redox behavior of the catalyst can neither be invoked here because, as has been described previously, the substituent (iPr or benzyl) of the oxazoline ligand has no apparent effect on the redox potentials. The significant influence of this substituent on the reactivity of the catalysts can then be explained by distinctive electronic effects that may tune the electrophilic/nucleophilic character of the intermediate species involved in the catalytic cycle, thus governing the preference for a less electron-rich substrate in the case of catalyst **3c**. This unusual reactivity difference depending on the substituents of the oxazolinic ligand led us to carry out a theoretical analysis of the reaction mechanisms for the different possible attacks to rationalize the reactivity differences observed.

Computational Results. We have initially performed DFT calculations on the geometry of **2c**, and the optimized structure obtained is overall in excellent agreement with the X-ray structure (rmsd 0.024 Å on distances and 0.8° on angles).³¹ As in previous similar studies,³² the DFT approach that we chose is able to offer reliable geometries of reactants, intermediates, and products. Starting from the Ru-oxo species obtained from the oxidation of the Ru–OH₂ complexes **3c** and **3'c** we analyzed the epoxidation at the different alkene sites of the 4-vinylcyclohexene substrate. Different epoxidized Ru-coordinated species

Table 5. Catalytic Performance of **3'c** and **3c** for the Epoxidation of *cis*- β -Methylstyrene and 4-Vinylcyclohexene Using $\text{PhI}(\text{OAc})_2$ as Oxidant^a

alkene \ complex	3'c		3c	
	Conversion (%)	Selectivity (%) ^b	Conversion (%)	Selectivity (%) ^b
	100	65 ^c	100	50 ^c
	74.1	75 (97.4 / 2.6) ^d	21.2	29 (0 / 100) ^d

^a Reaction conditions: catalytic oxidations were performed by dissolving the Ru-aqua complex (0.002 mmol) in degassed dichloromethane (2.5 mL) containing the alkene (0.2 mmol) and $\text{PhI}(\text{OAc})_2$ (0.4 mmol). The reaction mixture was stirred at RT for 24 h. After addition of an internal standard, an aliquot was taken for GC analysis. All the experiments have been done in the dark. ^b Selectivity for epoxide, [yield/conversion] \times 100. ^c For both catalysts 100% of *cis*-epoxide is obtained. ^d Ratio [ring epoxide/vinyl epoxide].

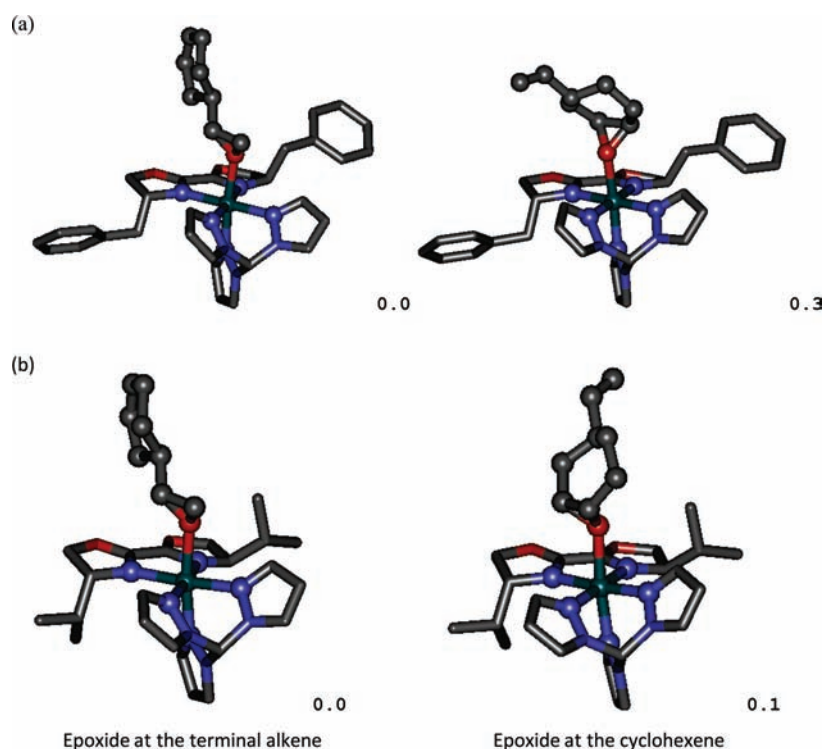


Figure 3. Relative energies (in kcal/mol) of the epoxidized Ru-coordinated species formed in the epoxidation of 4-vinylcyclohexene through either the terminal alkene or the ring by $[\text{Ru}^{\text{IV}}\text{O}(\text{tpm})(\text{R-box-C})]^{2+}$ complexes, R = Bz, 4'c (a) and R = iPr, 4c (b).

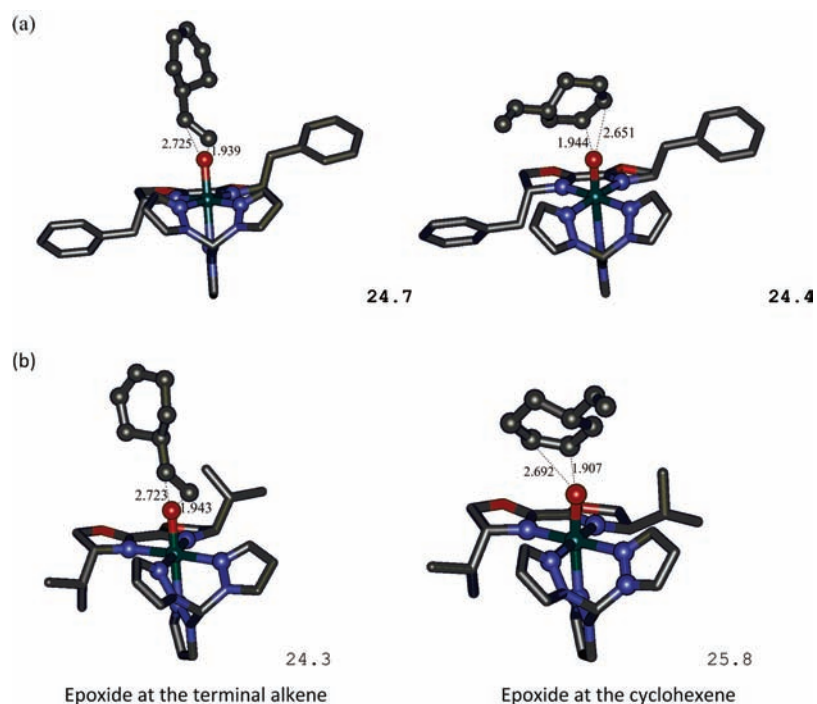


Figure 4. Transition states of the rate determining step with the main geometric parameters and energy barriers (in kcal/mol) for the epoxidation of 4-vinylcyclohexene through either the terminal alkene or the ring by $[\text{Ru}^{\text{IV}}\text{O}(\text{tpm})(\text{R-box-C})]^{2+}$ complexes, R = Bz, 4'c (a) and R = iPr, 4c (b).

corresponding to the two possible attacks and different conformations were obtained from which the most stable ones are collected in Figure 3. The BP86 calculated energy differences between the two possible products are so small (less than 0.3

kcal/mol) that they cannot be used to provide an explanation of the different behavior observed.

The formation of the epoxide at the terminal alkene is exergonic by 7.6 and 5.9 kcal/mol for 4'c (R = Bz) and 4c (R = iPr),

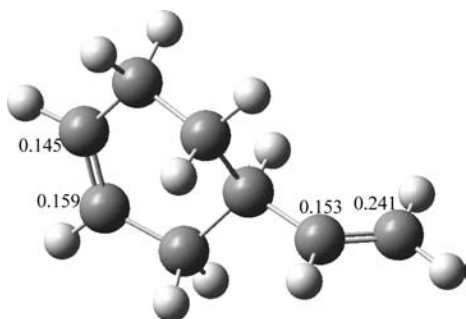


Figure 5. Condensed Fukui f^+ values on the 4-vinylcyclohexene.

respectively, with respect to the reactants, that is, the 4-vinylcyclohexene and the triplet oxo conformation of the corresponding $[\text{Ru}^{\text{IV}}\text{O}(\text{tpm})(\text{R-box-C})]^{2+}$ catalyst. The mechanism involves two steps. First the formation of a C–O bond, that is, the oxo group of the catalyst binds to one carbon atom of the attacked C=C double bond. This step involves the transition states (TS) displayed in Figure 4 that have in all cases a triplet ground state, the lowest-lying singlet excited state being about at least 5 kcal/mol higher in energy. The crossover from the singlet to the triplet surface should be possible through spin–orbit coupling. It is likely that the calculated barrier of about 25 kcal/mol for this step is somewhat overestimated, because the entropic contribution of the solute has been calculated in the gas-phase,³³ and it is well-known that ΔS_{rot} and ΔS_{trans} are larger in the gas-phase than in solution where rotation and translation are much more constrained.^{33b,34}

Overall, the different reactivity of $4'c$ and $4c$ can be discussed through the relative energy stability characterized by this first transition state (see Figure 4). For $4'c$ the interaction of the oxo species with the C=C double bond of the cyclohexene is favored by only 0.3 kcal/mol with respect to the C=C double bond of the terminal alkene. The barriers are 24.4 and 24.7 kcal/mol for the ring and terminal alkenes, respectively, calculated with respect to separated reactants. This is in line with the observed preference of $4'c$ for attacking the C=C double bond of the ring. The small difference between energy barriers concurs with the fact that some epoxidation occurs also on the terminal alkene (see Table 5). For $4c$ this energy difference increases to 1.5 kcal/mol (the barriers are 24.3 and 25.8 kcal/mol for the attack at the terminal alkene and the cyclohexene, respectively) and this agrees with the fact that $4c$ epoxidizes only the terminal alkene.

The intermediate species that result from the formation of the new C–O bond display a triplet ground state. For $4'c$, these intermediates are placed 22.4 and 23.3 kcal/mol higher in energy with respect to the final epoxidized species for the cyclic and terminal alkenes, respectively, whereas for $4c$ the corresponding values for ring and terminal epoxidation are in the order of 22.8 and 23.2 kcal/mol. Single-point energy calculations of these intermediates in the singlet state indicate that the singlet state is an excited state destabilized with respect to the triplet ground state by about 6 kcal/mol. All attempts to perform a geometry optimization of these intermediates with a singlet multiplicity led to the final epoxidized products in their singlet ground state. On the other hand, we have located the transition states that guide the formation of the epoxide, that is, the formation of the second C–O bond, in the triplet state surface. These TSs have energy barriers of about 16 and 19 kcal/mol for $4'c$ and $4c$, respectively. A single-point energy calculation of the singlet state at the

geometry of these TS shows that the singlet state is the ground state at this geometry and that it is stabilized by more than 25 kcal/mol with respect to the triplet state. Geometry optimizations of these transition states in the singlet state collapsed to the product. This means that once the intermediate crosses from the triplet to the singlet potential energy surface (a crossing that should take place near the triplet intermediate with an energy cost smaller than 6 kcal/mol and that should be possible through spin–orbit coupling), it evolves directly to the final product in a barrierless process. Therefore, the first step is the rate-determining step of the epoxidation process and is consequently the one that governs the selectivity of the epoxidation either on the terminal or the ring alkene.

We have also performed calculations of Fukui functions at the C=C double bonds of the substrate and at the oxo groups of both complexes. Fukui functions are useful to predict the reactivity of different atoms in a substrate toward a nucleophile or an electrophile.^{18,19} In principle the catalyst should attack nucleophilically, through the oxo group, one of the two C=C bonds of the substrate, that is, the study involves the calculation of the f^+ for the four carbon atoms contained in both alkene groups of the substrate. The f^+ values on the carbon atoms of the C–C double bonds are displayed in Figure 5. In average the terminal alkene displays higher regional Fukui functions toward a nucleophilic attack. On the other hand, when looking at the other agent, that is, the catalyst, we should pay attention to the f^- on the oxygen atom. The values of f^- are 0.013 and 0.105 for the catalysts containing benzyl and iPr groups, respectively. This important difference reveals that the system with iPr groups is significantly more nucleophilic.

From this static reactivity picture, one can conclude that the iPr system should have a larger preference for the C=C bond with the highest f^+ values from an electronic viewpoint. On the other hand, the benzyl system should be less selective and have more difficulties to distinguish, from an electronic point of view, between the two C=C double bonds. In fact, this agrees with the higher preference of the iPr system toward the terminal alkene.

CONCLUSIONS

We have synthesized a new family of Ru–OH₂ complexes where the alkylic iPr groups on the oxazolinic ligand do not have any remarkable influence on the spectroscopic and redox properties when compared to the analogous complexes containing Bz substituents but surprisingly determine a remarkable modification in the reactivity of these complexes toward the epoxidation of alkenes, with $3c$ being the first Ru catalyst capable to specifically epoxidize the terminal alkene of 4-vinylcyclohexene. The BP86 computed energy barriers of the first (and rate-determining) step corresponding to the interaction of the alkene groups with the catalytic systems bearing benzyl or isopropyl groups are in line with the different behavior observed in this regioselective epoxidation. Furthermore, calculations based on condensed Fukui functions reveal that the electronic factors play a key role and help to provide an explanation for the unexpected reactivity differences observed.

ASSOCIATED CONTENT

S Supporting Information. Additional spectroscopic, electrochemical data and full computational material, together with crystallographic information files. CIF for $2c$ and $2o$ have CCDC

nos. 827784 and 827785 respectively. This material is available free of charge via the Internet at <http://pubs.acs.org>. The supplementary crystallographic data can also be obtained free of charge via www.ccdc.cam.ac.uk/conts/retrieving.html (or from the Cambridge Crystallographic Data Centre, 12, Union Road, Cambridge CB2 1EZ, U.K.; fax +44 1223 336033 or E-mail deposit@ccdc.cam.ac.uk).

AUTHOR INFORMATION

Corresponding Author

*E-mail: marisa.romero@udg.edu (I.R.), montse.rodriguez@udg.edu (M.R.).

ACKNOWLEDGMENT

We acknowledge financial support from the MICINN of Spain (CTQ2010-21532-C02-01 to I.R. and M.R., CTQ2009-08328 to T.P., CTQ2010-21497 and Consolider Ingenio 2010 CSD2006-0003 to A.L. and CTQ2008-03077/BQU to M.S.) and the DIUE of Catalonia (2009SGR637). M.S. is also grateful to the DIUE of the Generalitat de Catalunya for financial help through the ICREA Academia 2009 prize for excellence in research. A.P. thanks MICINN for a Ramón y Cajal contract (ref RYC-2009-04170). Johnson & Matthey LTD are acknowledged for a $\text{RuCl}_3 \cdot n\text{H}_2\text{O}$ loan. We also thank Centre de Supercomputació de Catalunya (CESCA) for partial funding of computer time.

REFERENCES

- (1) (a) Sheldon, R. A.; Kochi, J. K. *Metal Catalyzed Oxidation of Organic Compounds*; Academic Press: New York, 1981. (b) Gamez, P.; Aubel, P. G.; Driessen, W. L.; Reedijk, J. *Chem. Soc. Rev.* **2001**, *30*, 376–385. (c) Robert, A.; Meunier, B. In *Biomimetic Oxidations Catalyzed by Transition Metal Complexes*; Meunier, B., Ed.; Imperial College Press: London, U. K., 2000; Chapter 12. (d) Bruijninx, P. C. A.; van Koten, G.; Gebbink, R. J. M. *Chem. Soc. Rev.* **2009**, *37*, 2716–2744.
- (2) (a) Ko, S. Y.; Lee, A. W. M.; Masamune, S.; Reed, L. A.; Sharpless, K. B.; Walker, F. J. *Science* **1983**, *220*, 949–951. (b) Nicolaou, K. C.; Winssinger, N.; Pastor, J.; Ninkovic, S.; Sarabia, F.; He, Y.; Vourloumis, D.; Yang, Z.; Li, T.; Giannakou, P.; Hamel, E. *Nature* **1997**, *387*, 268–272. (c) Gagnon, S. D. In *Encyclopedia of Polymer Science and Engineering*, 2nd ed.; Mark, H. F., Bikales, N. M., Overberger, C. G., Menges, G., Kroschwitz, J. I., Eds.; John Wiley & Sons: New York, 1985; Vol. 6, pp 273–307. (d) Darenbourg, D. J.; Mackiewicz, R. M.; Phelps, A. L.; Billodeaux, D. R. *Acc. Chem. Res.* **2004**, *37*, 836–844. (e) Jacobsen, E. N. *Catalysis Asymmetric Synthesis*; Ojima, I., Ed.; VCH: New York, 1993, 159.
- (3) (a) Bryant, J. R.; Matsuo, T.; Mayer, J. M. *Inorg. Chem.* **2004**, *43*, 1587–1592. (b) Sala, X.; Poater, A.; Romero, I.; Rodríguez, M.; Llobet, A.; Solans, X.; Parella, T.; Santos, T. M. *Eur. J. Inorg. Chem.* **2004**, 612–618. (c) Yip, W.-P.; Yu, W.-Y.; Zhu, N.; Che, C.-M. *J. Am. Chem. Soc.* **2005**, *127*, 14239–14249. (d) Zong, R.; Thummel, R. P. *J. Am. Chem. Soc.* **2005**, *127*, 12802–12803. (e) Poater, A.; Mola, J.; Saliner, A. G.; Romero, I.; Rodríguez, M.; Llobet, A.; Solà, M. *Chem. Phys. Lett.* **2008**, *458*, 200–204. (f) Mola, J.; Romero, I.; Rodríguez, M.; Bozoglian, F.; Poater, A.; Solà, M.; Parella, T.; Benet-Buchholz, J.; Fontrodona, X.; Llobet, A. *Inorg. Chem.* **2007**, *46*, 10707–10716. (g) Mola, J.; Rodríguez, M.; Romero, I.; Llobet, A.; Parella, T.; Poater, A.; Duran, M.; Solà, M.; Benet-Buchholz, J. *Inorg. Chem.* **2006**, *45*, 10520–10529.
- (4) (a) Stagni, S.; Orsellini, E.; Palazzi, A.; De Cola, L.; Zacchini, S.; Femoni, C.; Maccaccio, M.; Paolucci, F.; Zanarini, S. *Inorg. Chem.* **2007**, *46*, 9126–9138. (b) Murali, M.; Mayilmurugan, R.; Palaniandavar, M. *Eur. J. Inorg. Chem.* **2009**, 3238–3249. (c) Llobet, A. *Inorg. Chim. Acta* **1994**, *221*, 125–131. (d) Szczepura, L. F.; Maricich, S. M.; See, R. F.; Churchill, M. R.; Takeuchi, K. J. *Inorg. Chem.* **1995**, *34*, 4198–4205. (e) Mishra, D.; Barbieri, A.; Sabatini, C.; Drew, M. G. B.; Figgie, H. M.; Sheldrick, W. S.; Chattopadhyay, S. K. *Inorg. Chim. Acta* **2007**, *360*, 2231–2244. (f) Delaude, L.; Delfosse, S.; Richel, A.; Demonceau, A.; Noels, A. F. *Chem. Commun.* **2003**, 1526–1527.
- (5) Huynh, M. H. V.; Witham, L. M.; Lasker, J. M.; Wetzler, M.; Mort, B.; Jameson, D. L.; White, P. S.; Takeuchi, K. J. *J. Am. Chem. Soc.* **2003**, *125*, 308–309.
- (6) (a) Nishiyama, H.; Itoh, Y.; Matsumoto, H.; Park, S.-B.; Itoh, K. *J. Am. Chem. Soc.* **1994**, *116*, 2223–2224. (b) Jiang, Y.; Jiang, Q.; Zhang, X. *J. Am. Chem. Soc.* **1998**, *120*, 3817–3818. (c) Braunstein, P.; Fryzuk, M. D.; Naud, F.; Rettig, S. J. *J. Chem. Soc., Dalton Trans.* **1999**, 589–594. (d) Burguete, M. I.; Fraile, J. M.; García, J. I.; García-Verdugo, E.; Luis, S. V.; Mayoral, J. A. *Org. Lett.* **2000**, *2*, 3905–3908. (e) Ostergaard, N.; Jensen, J. F.; Tanner, D. *Tetrahedron* **2001**, *57*, 6083–6088. (f) McManus, H. A.; Guiry, P. J. *Chem. Rev.* **2004**, *104*, 4151–4202. (g) Le Mau, P.; Abrunhosa, I.; Berchel, M.; Simonneaux, G.; Gulea, M.; Masson, S. *Tetrahedron: Asymmetry* **2004**, *15*, 2569–2573. (h) Tse, M. K.; Klawonn, M.; Bhor, S.; Döbler, C.; Anilkumar, G.; Hugl, H.; Mägerlein, W.; Beller, M. *Org. Lett.* **2005**, *7*, 987–990.
- (7) (a) Hua, X.; Shang, M.; Lappin, A. G. *Inorg. Chem.* **1997**, *36*, 3735–3740. (b) Gómez, M.; Muller, G.; Rocamora, M. *Coord. Chem. Rev.* **1999**, *193–195*, 769–835. (c) Nishiyama, H.; Park, S.-B.; Haga, M.-A.; Aoki, K.; Itoh, K. *Chem. Lett.* **1994**, 1111–1114.
- (8) Rechavi, D.; Lemaire, M. *Chem. Rev.* **2002**, *102*, 3467–3493.
- (9) Serrano, I.; Sala, X.; Plantalech, E.; Rodríguez, M.; Romero, I.; Jansat, S.; Gómez, M.; Parella, T.; Stoekli-Evans, H.; Solans, X.; Font-Bardia, M.; Vidjayacoumar, B.; Llobet, A. *Inorg. Chem.* **2007**, *46*, 5381–5389.
- (10) Onishi, M.; Isagawa, K. *Inorg. Chim. Acta* **1991**, *179*, 155–156.
- (11) Hüchel, W.; Bretschneider, H. *Ber. Chem.* **1937**, *9*, 2024–2026.
- (12) Llobet, A.; Doppelt, P.; Meyer, T. J. *Inorg. Chem.* **1998**, *27*, 514–520.
- (13) Frisch, M. J.; Trucks, G. W.; Schlegel, H. B.; Scuseria, G. E.; Robb, M. A.; Cheeseman, J. R.; Scalmani, G.; Barone, V.; Mennucci, B.; Petersson, G. A.; Nakatsuji, H.; Caricato, M.; Li, X.; Hratchian, H. P.; Izmaylov, A. F.; Bloino, J.; Zheng, G.; Sonnenberg, J. L.; Hada, M.; Ehara, M.; Toyota, K.; Fukuda, R.; Hasegawa, J.; Ishida, M.; Nakajima, T.; Honda, Y.; Kitao, O.; Nakai, H.; Vreven, T.; Montgomery, Jr., J. A.; Peralta, J. E.; Ogliaro, F.; Bearpark, M.; Heyd, J. J.; Brothers, E.; Kudin, K. N.; Staroverov, V. N.; Kobayashi, R.; Normand, J.; Raghavachari, K.; Rendell, A.; Burant, J. C.; Iyengar, S. S.; Tomasi, J.; Cossi, M.; Rega, N.; Millam, N. J.; Klene, M.; Knox, J. E.; Cross, J. B.; Bakken, V.; Adamo, C.; Jaramillo, J.; Gomperts, R.; Stratmann, R. E.; Yazyev, O.; Austin, A. J.; Cammi, R.; Pomelli, C.; Ochterski, J. W.; Martin, R. L.; Morokuma, K.; Zakrzewski, V. G.; Voith, G. A.; Salvador, P.; Dannenberg, J. J.; Dapprich, S.; Daniels, A. D.; Farkas, Ö.; Foresman, J. B.; Ortiz, J. V.; Cioslowski, J.; Fox, D. J. *Gaussian 09*, Revision A.1; Gaussian, Inc.: Wallingford, CT, 2009.
- (14) (a) Becke, A. *Phys. Rev. A* **1988**, *38*, 3098–3100. (b) Perdew, J. P. *Phys. Rev. B* **1986**, *33*, 8822–8824. (c) Perdew, J. P. *Phys. Rev. B* **1986**, *34*, 7406–7406.
- (15) Schaefer, A.; Horn, H.; Ahlrichs, R. *J. Chem. Phys.* **1992**, *97*, 2571–2577.
- (16) (a) Haeusermann, U.; Dolg, M.; Stoll, H.; Preuss, H. *Mol. Phys.* **1993**, *78*, 1211–1224. (b) Kuechle, W.; Dolg, M.; Stoll, H.; Preuss, H. *J. Chem. Phys.* **1994**, *100*, 7535–7542. (c) Leininger, T.; Nicklass, A.; Stoll, H.; Dolg, M.; Schwerdtfeger, P. *J. Chem. Phys.* **1996**, *105*, 1052–1059.
- (17) (a) Barone, V.; Cossi, M. *J. Phys. Chem. A* **1998**, *102*, 1995–2001. (b) Tomasi, J.; Persico, M. *Chem. Rev.* **1994**, *94*, 2027–2094.
- (18) Parr, R. G.; Yang, W. *J. Am. Chem. Soc.* **1984**, *106*, 4049–4050.
- (19) (a) Yang, W.; Mortier, W. J. *J. Am. Chem. Soc.* **1986**, *108*, 5708–5711. (b) Poater, A.; Duran, M.; Jaque, P.; Toro-Labbé, A.; Solà, M. *J. Phys. Chem. B* **2006**, *110*, 6526–6536. (c) Costas, M.; Ribas, X.; Poater, A.; Valbuena, J. M. L.; Xifra, R.; Company, A.; Duran, M.; Solà, M.; Llobet, A.; Corbella, M.; Uson, M. A.; Mahia, J.; Solans, X.; Shan, X. P.; Benet-Buchholz, J. *Inorg. Chem.* **2006**, *45*, 3569–3581. (d) Ayers, P. W.; Parr, R. G. *J. Am. Chem. Soc.* **2000**, *122*, 2010–2018.

- (20) (a) Kohn, W.; Becke, A. D.; Parr, R. G. *J. Phys. Chem.* **1996**, *100*, 12974–12980. (b) Perdew, J. P.; Parr, R. G.; Levy, M.; Balduz, J. L. *Phys. Rev. Lett.* **1982**, *49*, 1691–1694.
- (21) (a) Reed, A. E.; Curtiss, L. A.; Weinhold, F. *Chem. Rev.* **1988**, *88*, 899–926. (b) Yang, W.; Parr, R. G.; Pucci, R. *J. Chem. Phys.* **1984**, *81*, 2862–2863.
- (22) (a) Sens, C.; Rodríguez, M.; Romero, I.; Parella, T.; Benet-Buchholz, J.; Llobet, A. *Inorg. Chem.* **2003**, *42*, 8385–8394. (b) Eskelinen, E.; Haukka, M.; Venäläinen, T.; Pakkanen, T.; Wasberg, M.; Chardon-Noblat, S.; Deronzier, A. *Organometallics* **2000**, *19*, 163–169. (c) Velders, A. H.; Hotze, A. C. G.; Ugolozzi, F.; Biagini-Cingi, M.; Manotti, A. M.; Haasnoot, J. G.; Reedijk, J. *Inorg. Chem.* **2000**, *39*, 3838–3844. (d) Serrano, I.; Rodríguez, M.; Romero, I.; Llobet, A.; Parella, T.; Campelo, J. M.; Luna, D.; Marinas, J. M.; Benet-Buchholz, J. *Inorg. Chem.* **2006**, *45*, 2644–2651. (e) Sala, X.; Poater, A.; von Zelewsky, A.; Parella, T.; Fontrodona, X.; Romero, I.; Solà, M.; Rodríguez, M.; Llobet, A. *Inorg. Chem.* **2008**, *47*, 8016–8024. (f) Sala, X.; Plantalech, E.; Romero, I.; Rodríguez, M.; Llobet, A.; Poater, A.; Duran, M.; Solà, M.; Jansat, S.; Gómez, M.; Parella, T.; Stoekli-Evans, H.; Benet-Buchholz, J. *Chem.—Eur. J.* **2006**, *12*, 2798–2807.
- (23) (a) Takeuchi, K. J.; Thompson, M. S.; Pipes, D. W.; Meyer, T. J. *J. Am. Chem. Soc.* **1984**, *23*, 1845–1851. (b) Leising, R. A.; Takeuchi, K. J. *Inorg. Chem.* **1987**, *26*, 4391–4393.
- (24) (a) Bessel, C. A.; Leising, R. A.; Takeuchi, K. J. *J. Chem. Soc. Chem. Commun.* **1991**, 883–835. (b) Dovletoglou, A.; Adeyemi, S. A.; Meyer, T. J. *Inorg. Chem.* **1996**, *35*, 4120–4127.
- (25) (a) Smith, J. G. *Synthesis-Stuttgart* **1984**, 629–656. (b) Schneider, C. *Synthesis-Stuttgart* **2006**, 3919–3944. (c) Weissermel, K. *Industrial Organic Chemistry*, 3rd ed.; VCH: Weinheim, Germany, 1997. (d) Xia, Q.-H.; Ge, H.-Q.; Ye, C.-P.; Liu, Z.-M.; Su, K.-X. *Chem. Rev.* **2005**, *105*, 1603–1662. (e) Che, C.-M.; Huang, J.-S. *Chem. Commun.* **2009**, 3996–4015. (f) Chatterjee, D. *Coord. Chem. Rev.* **2008**, *252*, 176–198. (g) Gupta, K. C.; Sutar, A. K.; Lin, C.-C. *Coord. Chem. Rev.* **2009**, *253*, 1926–1946.
- (26) (a) Sala, X.; Santana, N.; Serrano, I.; Plantalech, E.; Romero, I.; Rodríguez, M.; Llobet, A.; Jansat, S.; Gómez, M.; Fontrodona, X. *Eur. J. Inorg. Chem.* **2007**, 5207–5214. (b) Tse, M. K.; Bhor, S.; Klawonn, M.; Döbler, C.; Beller, M. *Tetrahedron Lett.* **2003**, *44*, 7479–7483.
- (27) (a) Tada, M.; Muratsugu, S.; Kinoshita, M.; Sasaki, T.; Iwasawa, Y. *J. Am. Chem. Soc.* **2010**, *132*, 713–724. (b) Yu, S.-Q.; Huang, J.-S.; Yu, W.-Y.; Che, C.-M. *J. Am. Chem. Soc.* **2000**, *122*, 5337–5342. (c) Stoop, R. M.; Bachmann, S.; Valentini, M.; Mezzetti, A. *Organometallics* **2000**, *19*, 4117–4126.
- (28) (a) Stultz, L. K.; Binstead, R. A.; Reynolds, M. S.; Meyer, T. J. *J. Am. Chem. Soc.* **1995**, *117*, 2520–2532. (b) Fung, W.-H.; Yu, W.-Y.; Che, C.-M. *J. Org. Chem.* **1998**, *63*, 7715–7726.
- (29) (a) Masllorens, E.; Rodríguez, M.; Romero, I.; Roglans, A.; Parella, T.; Benet-Buchholz, J.; Poyatos, M.; Llobet, A. *J. Am. Chem. Soc.* **2006**, *128*, 5306–5307. (b) Dakkach, M.; López, M. I.; Romero, I.; Rodríguez, M.; Atlamsani, A.; Parella, T.; Fontrodona, X.; Llobet, A. *Inorg. Chem.* **2010**, *49*, 7072–7079.
- (30) Kogan, V.; Quintal, M.; Neumann, R. *Org. Lett.* **2005**, *7*, 5039–5042.
- (31) Standard deviations for distances and angles: $s_{n-1} = [\sum_{i=1}^N (\text{CalcdVal}_i - \text{ExpVal}_i)^2 / (N - 1)]^{1/2}$, where CalcdVal means calculated value, ExpVal means experimental value (X-ray data), and N is the number of distances or angles taken into account (distances and angles used are given in the Supporting Information, Table S2). For examples, see: (a) Poater, A.; Cavallo, L. *Inorg. Chem.* **2009**, *48*, 4062–4066. (b) Duran, J.; Polo, A.; Real, J.; Benet-Buchholz, J.; Poater, A.; Solà, M. *Eur. J. Inorg. Chem.* **2003**, *414*, 4147–4151. (c) Poater, A. *J. Phys. Chem. A* **2009**, *113*, 9030–9040.
- (32) (a) Poater, A.; Ragone, F.; Correa, A.; Cavallo, L. *J. Am. Chem. Soc.* **2009**, *131*, 9000–9006. (b) Ragone, F.; Poater, A.; Cavallo, L. *J. Am. Chem. Soc.* **2010**, *132*, 4249–4258. (c) Bosson, J.; Poater, A.; Cavallo, L.; Nolan, S. P. *J. Am. Chem. Soc.* **2010**, *132*, 13146–13149. (d) Luan, X. J.; Mariz, R.; Gatti, M.; Costabile, C.; Poater, A.; Cavallo, L.; Linden, A.; Dorta, R. *J. Am. Chem. Soc.* **2008**, *130*, 6848–6858. (e) Poater, A.; Ragone, F.; Correa, A.; Szadkowska, A.; Barbasiewicz, M.; Grella, K.; Cavallo, L. *Chem.—Eur. J.* **2010**, *16*, 14354–14364. (f) Poater, A.; Cavallo, L. *J. Mol. Catal. A* **2010**, *324*, 75–79.
- (33) (a) Ardura, D.; Lopez, R.; Sordo, T. L. *J. Phys. Chem. B* **2005**, *109*, 23618–23623. (b) Leung, B. O.; Reid, D. L.; Armstrong, D. A.; Rauk, A. *J. Phys. Chem. A* **2004**, *108*, 2720–2725.
- (34) (a) Sakaki, S.; Takayama, T.; Sumimoto, M.; Sugimoto, M. *J. Am. Chem. Soc.* **2004**, *126*, 3332–3348. (b) Cooper, J.; Ziegler, T. *Inorg. Chem.* **2002**, *41*, 6614–6622. (c) Bieniek, M.; Michrowska, A.; Usanov, D. L.; Grella, K. *Chem.—Eur. J.* **2008**, *14*, 806–818.